Low Work Function Reduced Metal Complexes as Cathodes in Organic Electroluminescent Devices

Corey J. Bloom, C. Michael Elliott,* Paul G. Schroeder, C. Brian France, and B. A. Parkinson

Chemistry Department, Colorado State University, Fort Collins, Colorado 80523

Received: August 28, 2002; In Final Form: December 20, 2002

Several electrochemically active polypyridine-metal complexes are isolated in the formally zero-charged state via reductive electrocrystallization, and are thermally evaporated to form conducting thin films with low work functions. Solution-phase cyclic voltammetry of the parent complexes is used to predict the work function of these materials. The reduced films are used as cathode materials in organic light-emitting devices, in place of the commonly used low work function metals such as calcium and aluminum. These reduced complexes represent a new class of materials available for use as electron-injecting contacts in organic electroluminescent devices.

I. Introduction

Organic light-emitting devices (OLEDs) are composed of one or more thin layers of organic materials sandwiched between two conductors. An applied potential across the contacts injects electrons and holes from the cathode and anode, respectively. The charge carriers meet at a plane in the device, where they recombine to form an exciton. In a well-designed device, there is a high probability of photon emission from the excited state, as well as a balanced number of electrons and holes. Furthermore, the barrier to charge carrier injection at both electrode interfaces should be kept low to reduce power consumption. Since the pioneering work of Tang and VanSlyke,[1] much effort has focused on a general theme using tris(8-hydroxyquinoline) aluminum(III) complex (Alq_3) as the emissive and electron transport layer, and a triarylamine compound as the hole transport medium. The advantage of this approach lies in part in the emission of light at or near the interface between the two organic layers.

The exact mechanism for electron injection from the cathode into the adjacent organic layer is still a subject of debate, and likely differs depending on the exact nature of the device in question.[2,3] To a first approximation, a low barrier for injection should be provided when the Fermi energy of the cathode is closely matched to the lowest unoccupied molecular orbital (LUMO) energy of the emitting (or electron transport) layer. To this end, low work function (Φ) metals such as magnesium, calcium, and aluminum, or their alloys with silver are the most commonly used materials.[1,2,4] Advances have more recently been made utilizing very thin layers of insulators and wide band gap semiconductors between the conducting cathode and the active organic material. Specifically, inorganic insulators such as LiF, Li_2O, MgF_2, and MgO under aluminum metal have been widely used,[5−8] and copper phthalocyanine (CuPc) has been paired with the high work function conducting metal oxide indium tin oxide (ITO)[9] to produce a reasonably efficient transparent OLED. Doping of lithium metal into Alq_3 by codeposition has also been reported.[10]

Several arguments have been made to explain the success of these more complex systems. The formation of Li metal by reaction with Al has been proposed to explain the effect of LiF,[7] whereas others assert the mechanism is electron tunneling through the insulating salt[6,8] or band bending in the organic layer.[5] In a metal oxide on CuPc, the formation of midgap states due to damage by the deposition of the ITO onto the organic layer was thought to decrease the barrier to injection.[9] This latter result is particularly interesting, because there is no low work function material involved at all.

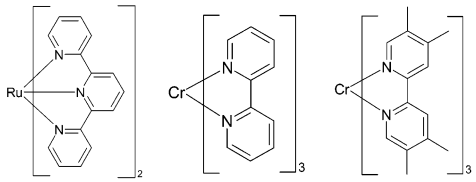

Figure 1. Structures of the metal complexes. (a) $[Ru(terpy)_2]^0$; (b) $[Cr(bpy)_3]^0$; (c) $[Cr(TMB)_3]^0$.

We recently reported a series of low Φ conducting polymers, one of which was used in conjunction with ITO as a cathode in an "inverted type" OLED.[11] The materials were composed of redox active substituted transition-metal diimine complexes, which as thin films were thermally polymerizable. Electrochemical reduction of the polymers yielded conductive films with work functions (which could be predicted from cyclic voltammetry of the monomers) from 3.7 to 3.0 eV. An OLED consisting of the layers gold/TPD/Alq_3/polymer/ITO was reported where gold was the anode. [TPD, *N*,*N*′-bis(3-methylphenyl-*N*,*N*′-diphenylbenzidine), is a commonly used organic hole transport material.] Although we were able to demonstrate that this type of device produces light under a moderate voltage bias, the performance was not optimal, most likely because of inherent limitations of the inverted geometry, the requirement of electrochemical reduction of the polymer, and the instability of the TPD/gold interface.[12] These problems made it difficult to draw definitive conclusions about the nature of the polymer/Alq_3 interface.

Here we introduce the use of a similar class of low Φ organic materials (LWOM) composed of redox active metal complexes, but ones that can be deposited by thermal evaporation (Figure 1a−c). Accordingly, these compounds are both simpler to use, and allow more flexible design of OLEDs. Devices of the type Metal/LWOM/Alq_3/TPD/ITO were constructed using silver and gold (both of which have relatively high Φ) in conjunction with the LWOM as a cathode, and their performance was evaluated.

10.1021/jp026865b CCC: $25.00
Published on Web 03/11/2003

II. Experimental Section

Chemicals. Acetonitrile was Aldrich Optima grade, stored over 4 Å molecular sieves, and distilled from CaH_2. Ammonium hexafluorophosphate ($NH_4^+PF_6^-$) was supplied by Elf Atochem and tetra-*n*-butylammonium hexafluorophosphate ($TBA^+PF_6^-$) electrolyte was prepared as described elsewhere.[13] The ligand 4,4′,5,5′-tetramethyl-2,2′-bipyridine (TMB) was produced by a coupling reaction of 3,4-lutidine (Aldrich) over Pd on C, followed by recrystallization from ethyl acetate. 2,2′-Bipyridine (bpy) was purchased from Baker, and 2,2′:6′,2″-terpyridine (terpy) from Aldrich, and both were used without further purification. Alq_3 and TPD, from Aldrich, were purified by vacuum train sublimation with Argon gas flow at 330 °C and 270 °C, respectively. Chromic chloride was supplied by Fisher. Gold of purity 99.99% was purchased from Alfa Aesar, and 99.9999% pure silver from Sargent-Welch. The conducting polymer dispersion, poly(styrenesulfonate)-poly(2,3-dihydrothieno-[3,4-*b*]-1,4-dioxin) 1.3 wt % in H_2O (PEDOT-PSS), was supplied by Aldrich. ITO, 4−8 Ω/sq. on glass, was purchased from Delta Technologies, Ltd.

Synthesis of $[Ru(terpy)_2]^{2+}(PF_6^-)_2$. Terpyridine (100 mg, 0.429 mmol) in 10 mL ethylene glycol was added to $Ru(DMSO)_4Cl_2$ (95 mg, 0.196 mmol) in 4 mL 1:1 methanol/water. The mixture was heated under N_2 via an oil bath held at 100 °C for 2.5 h, producing a dark reddish solution which was then cooled to room temperature. Water was added to reach a total volume of 75 mL and $NH_4^+PF_6^-$ was added whereupon a red/orange precipitate formed. The solid was washed well with H_2O and recrystallized from methanol to yield brick red crystals.

Synthesis of $[Cr(bpy)_3]^{3+}(ClO_4^-)_3$. A procedure modified from the literature was used.[14,15] $CrCl_3 \cdot 6H_2O$ (1.33 g, 0.0050 mol) was refluxed under N_2 in 0.05 M $HClO_4$ (Mallinckrodt) over Al metal (Baker) to produce a blue/green solution likely containing both Cr^{2+} and Cr^{3+}. This solution was added to a N_2-purged suspension of bpy (7.81 g, 0.050 mol) in aqueous $HClO_4$ of pH 2. A black suspension was quickly formed, which slowly turned yellow {indicating formation of the $[Cr(bpy)_3]^{3+}$ complex} upon bubbling with O_2 for 2 h. The yellow solid was collected by filtration, washed well with water, ethanol, and CH_2Cl_2 (to remove excess ligand), and finally recrystallized from water.

Synthesis of $[Cr(TMB)_3]^{3+}(ClO_4^-)_3$. The procedure above was changed only slightly, using much less TMB ligand (0.50 g), because in this case the large excess proved unnecessary and difficult to remove, and 0.285 g chromic chloride. The resulting yellow solid was washed with ethanol and boiling hot water.

Electrochemistry. Cyclic voltammetry was performed in a Luggin capillary cell with a Ag/Ag^+ 0.1 M in dimethyl sulfoxide (DMSO) [0.41 V vs normal hydrogen electrode (NHE)] reference electrode, Pt wire counter, and glassy carbon working electrode, in 0.1 M $TBA^+PF_6^-$ in CH_3CN electrolyte. The scan rate was 50 mV/s. Electronics consisted of a P.A.R. model 173 Potentiostat and model 175 Programmer with output to a Yokogawa X/Y recorder.

Electrocrystallization. The three complexes were electrocrystallized following a modification of a method described in the literature.[16,17] A three-compartment bulk electrolysis cell was used in an inert atmosphere glovebox with the same electrolyte, reference, and counter electrodes as above, and a Pt mesh working electrode (WE). To produce $[Ru(terpy)_2]^0$, 50 mg of $[Ru(terpy)_2]^{2+}(PF_6^-)_2$ was added to the WE compartment, and vigorously stirred. The WE was held at a constant potential of −2.00 V (several hundred millivolts past the second reduction as determined from cyclic voltammetry) until the current decayed from approximately 500 mA to less than 100 μA during the course of several hours. The WE, which was covered with purple/black crystals of the reduced complex, was disconnected from the potentiostat and removed from the electrolysis solution. These crystals were dislodged from the WE in fresh CH_3CN, collected on a fritted filter, and washed with more acetonitrile. The solid was dried by passage of glovebox atmosphere over the solid with a vacuum pump, and scraped into a boat for thermal deposition. Crystals of $[Cr(bpy)_3]^0$ and $[Cr(TMB)_3]^0$ were prepared in the same manner, but at controlled potentials of −1.90 V and −2.15 V vs Ag/Ag^+ 0.1 M in DMSO, respectively.

Photoelectron Spectroscopy. All photoelectron spectroscopy work was performed in an Omicron multiprobe UHV chamber (base pressure 5×10^{-11} Torr) equipped with a VSW EA125 single-channel analyzer. A transfer rod assembly was used which could be moved into the glovebox for sample preparation, and the sample isolated from the atmosphere behind a gate valve. This assembly was affixed to the entry chamber of the UHV system and pumped down to vacuum before introducing the sample into the analysis chamber. The X-ray source was the Mg Kα line at 1253.6 eV. The UV light source was a helium arc lamp, providing a He(I) line at 21.22 eV and a He(II) line at 40.81 eV. A −5.00 V bias was applied to the sample to separate the spectrometer and sample high binding energy cutoffs. Kinetic energy analysis of electrons emitted normal to the sample was done using a 10 eV pass energy. The spectrometer was calibrated with an Ar^+ ion sputtered copper standard.

A straight line was fit on the secondary edge of the UPS He(I) spectrum (and the XPS spectrum). The intercept of this line with the abscissa determines the high binding energy cutoff (HBEC). A value of 0.1 eV was subtracted from the HBEC to correct for spectrum broadening due to thermal and analyzer effects.[18] The work function was determined by subtracting this value from the source energy of 21.22 eV.

OLED Construction. After rinsing in ethyl acetate and isopropyl alcohol, patterned ITO substrates were cleaned in a laminar flow hood by successive sonication in a 5% aqueous solution of VWR aquasonic cleaner followed by Millipore water. For devices including PEDOT-PSS, the polymer suspension was filtered through a 0.2-μm cellulose acetate syringe filter (Nalgene) and spin coated onto an ITO substrate at approximately 1000 rpm using a modified commercial blender.[11] The substrates were introduced first into the glovebox and then the vacuum deposition chamber (Denton DV 502A Turbo model) that is directly interfaced with the glovebox. Organic materials and metals were sequentially deposited at pressures below 3×10^{-6} Torr. The thickness of the various layers was measured by a Leybold Inficon quartz crystal microbalance and XTM-2 Deposition Monitor. Device testing was performed using a Kiethley 2400 Sourcemeter and Newport 1830-C Optical Power Meter with 818-SL Photodiode detector driven by LabVIEW 6.0 Software.

III. Background and Theory

To expand the range of materials available for use as cathodes for OLEDs, and possibly to understand better the nature of the conductor/organic interface, we previously introduced a series of conducting polymers with low work functions.[11] The thin polymer films were composed of substituted tris(bipyridine) ruthenium(II) complex monomers, which by nature have many closely spaced (in potential) redox couples at negative potentials.

Electrochemical reduction of the active sites in the polymer to the formally zero-charged state afforded electronically conductive (resistivity $\rho \sim 1 \times 10^3$ Ω·cm) low Φ films.[11,19] The conductivity and low work functions are both explained by considering the consequences of the proximal redox processes, as predicted by the Nernst equation. Because of thermal energy, at least three oxidation states (1+, 0, and 1−, where the charged species are present in equal numbers) are present in moderate concentration at room temperature in the reduced films. Furthermore, because the LUMO energy of the free ligands can be controlled by synthetic alterations, the Φ of the resulting reduced films can be tuned. Photoelectron spectroscopy was used to verify that the Φ could be predicted by cyclic voltammetry of the monomers in solution from the average of the $E_{1/2}$ of the 1+/0 and 0/1− couples.[11]

In principle, the same factors that apply to the conductivity and Φ of the previously described polymers should also apply to solids composed of neutral small-molecule organics with similar redox properties. Moreover, because in certain cases these materials can be thermally vapor deposited, they would provide some important advantages over the polymers in OLED applications. By eliminating the necessity of postpolymerization electrochemical processing, small-molecule LWOMs would allow a much greater variety of device architectures, and no doubt would be inherently more pure. Redox active polypyridine complexes of transition metals are a natural choice, in that they possess numerous oxidation states with small voltage separations. Neutral complexes can be produced by electrochemical or chemical reduction of the complex, by adding a number of electrons equal to the initial positive charge. Also, by virtue of a lack of formal charge, isolation of the zero-valent form is often simple because of the different solubility than the charged species.

The solid-state compounds $[Ru(bpy)_3]^0$ and $[Ru(terpy)_2]^0$, prepared by reductive electrocrystallization from the 2+ species, have been studied recently as interesting electronic systems.[16,17,20] The conductivity of single-crystalline $[Ru(bpy)_3]^0$ was reported as $\sigma \sim 1.5 \times 10^{-1}$ Ω^{-1} cm^{-1} at 297 K, with a semiconductor-like temperature coefficient.[21] Based on the conductivity, X-ray crystal structures, electron paramagnetic resonance, and magnetic properties of these systems, several possible models for the electronic structure (and thus mode of conduction) were proposed. In the simplest case, the two "extra" electrons provided by the reduction are seen as localized on individual ligands, but can undergo very facile intra- *and* intermolecular exchange due to efficient orbital overlap.[21] Alternately, an "expanded atom" model was considered that treats the electrons as a completely delocalized pseudospherical ligand around the cationic core.[22] Finally, the more extreme possibility of an "electride"[23] was discussed, in which the electrons are essentially altogether freed from the complexes and exist as a "lattice gas," residing in cavities within the crystal lattice.[17,20] A definitive argument for any one of these models was not made, and it may be most appropriate to view these cases as three points along a continuum of electronic structure. Regardless of the actual mechanism, electrons in these systems clearly are fairly mobile; and although conductivity has been reported only for the bpy complex as a single crystal, it is reasonable to expect that thin polycrystalline or amorphous films of either species would also be respectable conductors.

Extrapolating from the results with these neutral ruthenium complexes, one might expect $[Cr(bpy)_3]^0$ to also be conductive given its similar reduction electrochemistry. Although the solid-state conductivity of this system has not been reported, analysis of the electron-transfer reaction between $[Cr(bpy)_3]^{1+}$ and $[Cr(bpy)_3]^0$ in *N*,*N*-dimethylformamide solution revealed a very fast second-order rate constant of 2.0×10^9 M^{-1} s^{-1}.[24] This rate was rationalized in part by minimal inner-sphere reorganization upon electron exchange, which would be expected for all of these complexes, and would also be consistent with facile electron transfer in the solid state.

Attempts to vapor deposit $[Ru(bpy)_3]^0$ were unsuccessful; however, both $[Ru(terpy)_2]^0$ and $[Cr(bpy)_3]^0$ could be deposited at moderate temperatures and pressures below 6×10^{-6} Torr. Using the ligand-localized electron model, we attribute this difference in behavior to the symmetry of these neutral complexes. When each added electron is assumed to be instantaneously localized on a single ligand, the symmetry of $[Ru(bpy)_3]^0$, $[Ru(terpy)_2]^0$, and $[Cr(bpy)_3]^0$ are, respectively, C_2, D_{2d}, and D_3. Although all three complexes are uncharged, the point groups of the latter two species do not permit a dipole, whereas $[Ru(bpy)_3]^0$ in C_2 can, and presumably does, have a dipole. Moreover, if the electron were totally localized, the instantaneous dipole is predicted to be quite large (on the order of 20 D). Presumably a strong dipolar interaction in the solid significantly reduces the volatility of $[Ru(bpy)_3]^0$ relative to the other reduced complexes that both lack dipoles. This pattern indicates a further constraint for complexes to use as evaporable LWOMs: when the reductions are essentially ligand based, the number of ligands must be equal to the initial positive charge on the complex and therefore the number of electrons by which it is reduced. Regarding the models of electronic structure considered above, this result is particularly at odds with the expanded atom view, and most consistent with the localized electron description.

To predict (via cyclic voltammetry) the Φ of "zero-valent" polymeric materials reported earlier, we presented a model assuming discrete redox sites having 1+, 0, and 1− oxidation states and an overall neutral charge. This is conceptually analogous to a narrow band gap intrinsic semiconductor, with a large (*and equal*) number of electrons and holes produced by thermal excitation. In this picture, the Fermi level (E_F) should lie in the middle of the band gap. Accordingly, the E_F can be estimated as the average potential for the redox processes creating the two singly charged species, and by extension the Φ can be calculated.[11] In light of the more complex electronic models discussed above for the small-molecule LWOMs considered here, the assumption of isolated charged sites is likely not entirely valid in a more ordered crystalline environment. Nonetheless, the energy levels of the reductions (i.e., $E_{1/2}$ $[Ru(terpy)_2]^{1+/0}$ and $E_{1/2}$ $[Ru(terpy)_2]^{0/1-}$), provided by cyclic voltammetry, should yield at least a rough estimate of the energy of electrons in the solid LWOMs.

IV. Results and Discussion

From cyclic voltammetry (Figure 2 and literature[25]), the $E_{1/2}$ for the reductions along with calculated E_F and Φ, of $[Ru(terpy)_2]^0$, $[Cr(bpy)_3]^0$, and $[Cr(TMB)_3]^0$ are presented in Table 1. Note that, as predicted, the TMB complex undergoes reductive processes at potentials significantly more negative than does the bpy analogue because of the electron-donating nature of the methyl substituents on the ligands. Indeed, for this system, the fourth reduction (0/1−) is outside the electrochemical window available in acetonitrile solvent and must be estimated by comparison to the other Cr complex. This seems to be a fair assessment, because the three corresponding measured reductions are each shifted by approximately the same amount. The data were obtained using either a Ag/Ag^+ 0.1 M in DMSO or

TABLE 1: $E_{1/2}$ Potentials for Reductions of Metal Complexes. Conditions for Cyclic Voltammetry of Cr Complexes: Electrolyte, 0.1 M $TBAPF_6$ in CH_3CN; WE, Glassy C; CE, Pt Wire; Scan Rate, 100 mV/s

	$E_{1/2}$ vs Ag/Ag^+ 0.1 M in DMSO, V				$E_{1/2}$ vs NHE, V			
	3+/2+	2+/1+	1+/0	0/1−	1+/0	0/1−	E_F calc., eV	Φ calc., eV
$Ru(terpy)_2$		−1.44*	−1.69*	−2.13*	−1.28	−1.72	−1.50	3.10
$Cr(bpy)_3$	−0.48	−0.98	−1.56	−2.18	−1.15	−1.77	−1.46	3.14
$Cr(TMB)_3$	−0.72	−1.25	−1.85	−2.46**	−1.44	−2.05**	−1.75	2.85

* Values from the literature were originally reported vs SSCE[25] but have been converted for this table. ** Estimated by comparison with bpy complex.

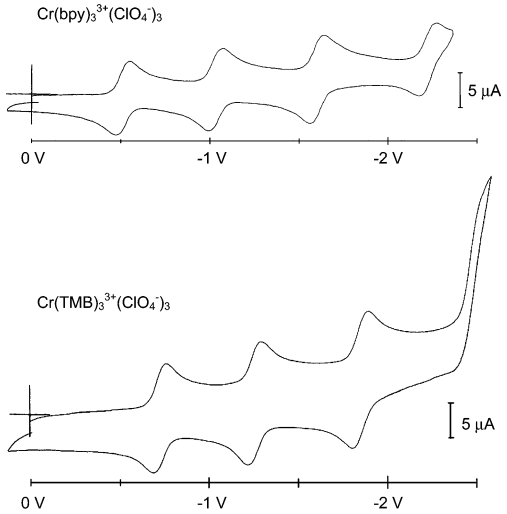

Figure 2. Cyclic voltammetry of the Cr complexes. The fourth reduction of the $Cr(TMB)_3$ complex is obscured by the solvent window.

saturated sodium chloride calomel (SSCE) reference electrode. Potentials are also reported relative to the standard electrode for electrochemical data, the NHE, by subtracting the difference in potential of the reference electrode used in the experiment from that of the NHE, 0.410 and 0.236 V, respectively. The E_F vs NHE is calculated as the average of the half-wave potentials for the 1+/0 and 0/1− reductions, and finally the Φ is estimated by comparison of the energy of the NHE to the energy of a free electron in a vacuum, −4.60 eV.[26]

X-ray and ultraviolet photoelectron spectroscopy (XPS and UPS) were performed on a 200-Å-thick film of $[Ru(terpy)_2]^0$ thermally deposited on Pt foil. XPS spectra (see Supporting Information) revealed the presence of carbon, nitrogen, and ruthenium, as expected, as well as oxygen. Although the films were prepared and transferred to the UHV chamber under an inert atmosphere, it is possible that a small amount of O_2 did contact the reduced LWOM in the transfer process. The work function of the film was measured from the HBEC (see Experimental Section) to be 3.32 and 3.38 eV, by XPS and UPS, respectively (spectra are in Supporting Information). These values, while in good agreement with each other, are slightly higher than the value of 3.10 eV predicted from the electrochemical data and are not as close to the predicted Φ as are the values obtained for similar conducting polymers.[11] The difference from the predicted value could be rationalized in several ways; by a partial oxidation of the films while moving the sample into the UHV chamber, by solid-state effects in the crystal lattice, or by delocalization of electron density. Extensively delocalized electrons in the solid, in the model of an electride, would likely reside at a lower energy than electrons in a corresponding isolated complex. This should result in a somewhat lower E_F, and thereby a greater work function. Aside from any such delocalization effects, the ordering of complexes in a crystalline environment could change the highest occupied and lowest unoccupied molecular orbital energies (relative to the energies of an isolated complex in soloution) in a systematic fashion. In contrast, the energies in an amorphous polymer environment, like those reported previously,[11] should be more randomly distributed about the value for an isolated unit. In

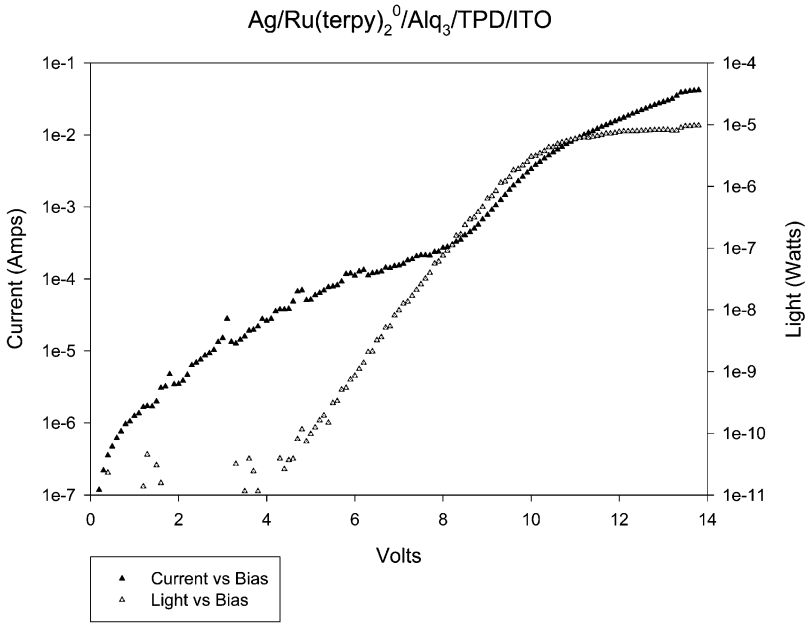

Figure 3. Performance of a typical OLED with a $[Ru(terpy)_2]^0$/Ag cathode.

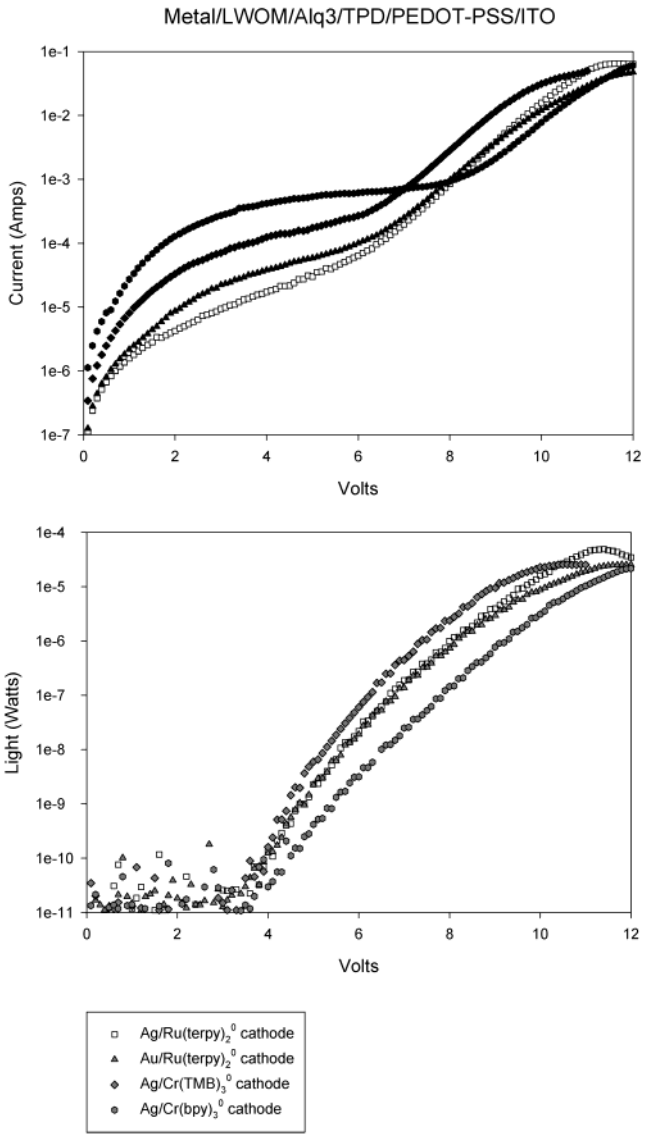

Figure 4. Performance of four OLEDs with cathodes of varying LWOMs and covering metal layers.

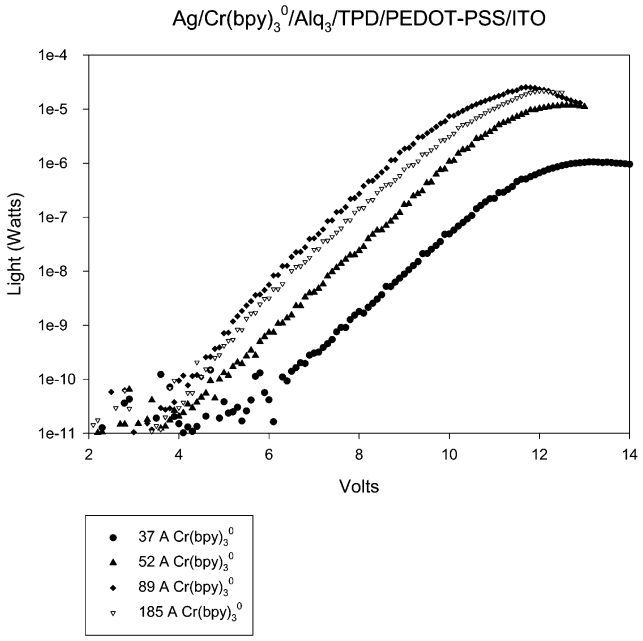

Figure 5. Performance of OLEDs with $[Cr(bpy)_3]^0$/Ag cathodes with increasing thickness of $[Cr(bpy)_3]^0$.

any case, the Φ for $[Ru(terpy)_2]^0$ provided by photoelectron spectroscopy is within the range of commonly used metals for OLED cathodes (by comparison, Ca metal has a Φ of 2.9 eV), and is at least fairly close to the predicted value of 3.10 eV.

First-generation OLEDs were constructed using $[Ru(terpy)_2]^0$ with the architecture Ag/LWOM/Alq_3(400 Å)/TPD(400 Å)/ITO. Performance for a typical device with $[Ru(terpy)_2]^0$ as the LWOM is shown in Figure 3. Emission spectra for these devices peak in the 520 nm region typical of Alq_3-based devices, and there is no evidence of emission from the LWOM layer.

A second generation of devices was prepared including a conducting polymer interlayer (PEDOT-PSS) between the ITO anode and the TPD hole-transport material. This approach has been shown to improve device performance by reducing the barrier to hole injection at the anode,[27,28] resulting in increased device lifetime and efficiency. Devices containing this additional layer for hole injection both passed more current and produced more light at a given voltage, as shown in Figure 4.

To investigate the role of the metal layer covering the LWOM, analogous OLEDs were also made with gold, which has a very high Φ of 5.2 eV.[3] Devices with architecture Au/LWOM/Alq_3(400 Å)/TPD(200 Å)/PEDOT-PSS/ITO performed very similarly to those with silver (see Figure 4). This observation supports the assertion that the nature of the metal contact is of secondary importance to the underlying LWOM. In contrast, when devices are constructed in exactly the same manner, but omitting the LWOM layer, they emit only weakly and at high voltages with Ag metal cathodes and not at all when Au is used. "Hole only" devices *without* Alq_3 also were constructed, consisting of the layers ITO/ PEDOT-PSS/TPD (800 Å)/$Ru(terpy)_2^0$/Metal, with both Ag and Au metals. The current/voltage response of such devices (shown in supporting material) with the two metals was very similar, and unlike in OLEDs including Alq_3, the current passed at bias greater than about 3 V appeared to be essentially ohmic.

Figure 4 also depicts the performance of OLEDs with $[Cr(TMB)_3]^0$ and $[Cr(bpy)_3]^0$ as the cathode materials. A device using the TMB complex emits more light, while passing more current, than does a comparable device containing $[Ru(terpy)_2]^0$. This may be attributed to the lower calculated Φ of the reduced complex, which would be expected to yield a lower barrier for electron injection. On the other hand, devices using $[Cr(bpy)_3]^0$ produce noticeably less light emission than do those with $[Ru(terpy)_2]^0$, which cannot be easily explained on the basis of the predicted work function alone. External quantum efficiencies ($\varphi_{ext.}$) of OLEDs containing $[Ru(terpy)_2]^0$ with silver and gold, as well as $[Cr(TMB)_3]^0$, are at a maximum of 0.04−0.05% at 8 V bias. Devices with $[Cr(bpy)_3]^0$ based cathodes have a significantly lower maximum $\varphi_{ext.}$ at 10 V bias of only 0.02%.

Notably, the performance of OLEDs having a relatively thick layer of LWOM is superior to those with thin layers (i.e. < 100 Å). This is in contrast to what was observed for more insulating materials such as inorganic salts[5,7,8] and CuPc,[9] where only very thin layers of less than 50 Å are effective. Light emission from several devices differing only in the thickness of LWOM is displayed in Figure 5. The OLEDs having thicker layers (89 or 185 Å) of $[Cr(bpy)_3]^0$ produce several orders of magnitude more light than do those with only 37 Å.

By closer analysis of the I−V curves, it is possible to gain a deeper understanding of the nature of the electron-injection process in these devices. Several models have been developed to account for charge injection and transport in OLEDs that are identified by the shape of the current−voltage curves. For

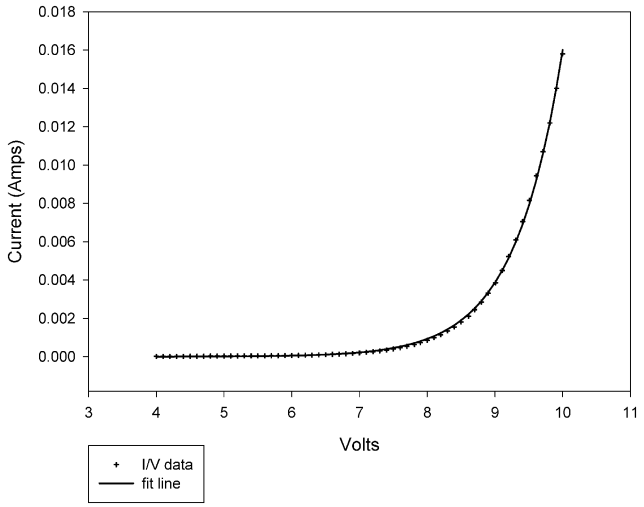

Figure 6. Current−voltage performance of an OLED of construction Ag/ $[Ru(terpy)_2]^0$/Alq_3/TPD/PEDOT-PSS/ITO (as shown in Figure 4) and a fit to the equation $I \propto e^{cV}$.

devices governed by trap-limited electron conduction in the Alq_3 layer, the power law equation $I \propto V^{m-1}$ (where *m* is typically 7−9) describes the I−V relationship.[2] In this case, the current is limited by transport characteristics of the Alq_3, rather than a barrier to injection at the interface with the cathode. For the OLEDs constructed here, fits to the power law relation have been unsatisfactory, whereas an exponential dependence of I on V is well obeyed. The I−V performance, in the useful operating range of 4−10 V, of the previously discussed $[Ru(terpy)_2]^0$ containing device (with PEDOT-PSS), along with the exponential relationship $I \propto e^{cV}$ is shown in Figure 6. This suggests that these devices are governed not by trap-limited conduction in the Alq_3, but rather by an injection-limited mechanism.

V. Conclusions

We have introduced a class of electrochemically active transition metal complexes that can be reduced and isolated in a conductive zero-charged form. In this state these materials are suitable for use as electron-injecting contacts in OLEDs using the common emitting material Alq_3. Although the mechanism for electron injection from these layers into Alq_3 is not yet fully understood, the identity of the material contacting these relatively thick conducting organic layers clearly has only a very minor effect on device performance. This allows the use of air-stable metals such as silver or gold for contacts covering the LWOM layers. It should be further possible to replace the metal with a transparent conducting oxide such as ITO, yielding a completely transparent device.

Acknowledgment. The authors gratefully acknowledge support from the NSF, grant number CHE-0139637 (C.M.E.), and DOE-BES contract DE-FG03-96ER14625 (B.A.P.).

Supporting Information Available: XPS spectra and I/V plots. This information is available free of charge via the Internet at http://pubs.acs.org.

References and Notes

(1) Tang, C. W.; VanSlyke, S. A. *Appl. Phys. Lett.* **1987**, *51*, 913.
(2) Burrows, P. E.; Forrest, S. R. *Appl. Phys. Lett.* **1994**, *64*, 2285.
(3) Parker, I. D. *J. Appl. Phys.* **1994**, *75*, 1656.
(4) Matsumura, M.; Akai, T.; Saito, M.; Kimura, T. *J. Appl. Phys.* **1996**, *79*, 264.
(5) Hung, L. S.; Tang, C. W.; Mason, M. G. *Appl. Phys. Lett.* **1997**, *70*, 152.
(6) Jabbour, G. E.; Kawabe, Y.; Shaheen, S. E.; Wang, J. F.; Morrell, M. M.; Kippelen, B.; Peyghambarian, N. *Appl. Phys. Lett.* **1997**, *71*, 1762.
(7) Matsumura, M.; Jinde, Y. *Appl. Phys. Lett.* **1998**, *73*, 2872.
(8) Lee, C. H. *Synth. Met.* **1997**, *91*, 125.
(9) Parthasarathy, G.; Burrows, P. E.; Khalfin, V.; Kozlov, V. G.; Forrest, S. R. *Appl. Phys. Lett.* **1998**, *72*, 2138.
(10) Kido, J.; Matsumoto, T. *Appl. Phys. Lett.* **1998**, *73*, 2866.
(11) Bloom, C. J.; Elliott, C. M.; Schroeder, P. G.; France, C. B.; Parkinson, B. A. *J. Am. Chem. Soc.* **2001**, *123*, 9436.
(12) Bulovic, V.; Tian, P.; Burrows, P. E.; Gokhale, M. R.; Forrest, S. R.; Thompson, M. E. *Appl. Phys. Lett.* **1997**, *70*, 2954.
(13) Elliott, C. M.; Redepenning, J. G. *J. Electroanal. Chem.* **1986**, *197*, 219.
(14) Pecsok, R. L.; Lingane, J. L. *J. Am. Chem. Soc.* **1950**, *72*, 189.
(15) Baker, B. R.; Mehta, B. D. *Inorg. Chem.* **1965**, *4*, 848.
(16) Perez-Cordero, E.; Buigas, R.; Brady, N.; Echegoyen, L. *Helv. Chim. Acta* **1994**, *77*, 1222.
(17) Pyo, S.; Perez-Cordero, E.; Bott, S. G.; Echegoyen, L. *Inorg. Chem.* **1999**, *38*, 3337.
(18) Schlaf, R.; Schroder, P. G.; Nelson, M. W.; Parkinson, B. A.; Merritt, C. D.; Crisafulli, L. A.; Murata, H.; Kafafi, Z. H. *Surf. Sci.* **2000**, *450*, 142.
(19) Elliott, C. M.; Redepenning, J. G.; Balk, E. M.; Schmittle, S. J. *Electronically Conducting Films of Poly(trisbipyridine)-Metal Complexes*; ACS Symposium Series 360 (Inorganic and Organometallic Polymers); American Chemical Society: Washington, DC, 1988.
(20) Perez-Cordero, E.; Campana, C.; Echegoyen, L. *Angew. Chem., Int. Ed. Engl.* **1997**, *36*, 137.
(21) Wagner, M. J.; Dye, J. L.; Perez-Cordero, E.; Buigas, R.; Echegoyen, L. *J. Am. Chem. Soc.* **1995**, *117*, 1318.
(22) Echegoyen, L.; Xie, Q.; Perez-Cordero, E. *Pure Appl. Chem.* **1993**, *65*, 441.
(23) Dye, J. L. *Inorg. Chem.* **1997**, *36*, 3816.
(24) Saji, T.; Aoyagui, S. *Bull. Chem. Soc. Jpn.* **1973**, *46*, 2101.
(25) Morris, D. E.; Hanck, K. W.; DeArmond, M. K. *J. Electroanal. Chem.* **1983**, *149*, 115.
(26) Trasatti, S. *Pure Appl. Chem.* **1986**, *58*, 955.
(27) Troadec, D.; Veriot, G.; Antony, R.; Moliton, A. *Synth. Met.* **2001**, *124*, 49.
(28) Elschner, A.; Bruder, F.; Heuer, H. W.; Jonas, F.; Karbach, A.; Kirchmeyer, S.; Thurm, S.; Wehrmann, R. *Synth. Met.* **2000**, *111*−*112*, 139.